Letter

Electronic correlations in the ultranarrow energy band compound $Pb_9Cu(PO_4)_6O$: A DFT+DMFT study

Dmitry M. Korotin [1,2,*] Dmitry Y. Novoselov [1,2,3] Alexey O. Shorikov [1,2,3]
Vladimir I. Anisimov [1,2,3] and Artem R. Oganov [2,4]

[1]*M. N. Mikheev Institute of Metal Physics of the Ural Branch of the Russian Academy of Sciences, 18 S. Kovalevskaya Street, Yekaterinburg 620108, Russia*
[2]*Skolkovo Institute of Science and Technology, 30 Bolshoy Boulevard, Building 1, Moscow 121205, Russia*
[3]*Department of Theoretical Physics and Applied Mathematics, Ural Federal University, 19 Mira Street, Yekaterinburg 620002, Russia*
[4]*Moscow Institute of Physics and Technology, 9 Institutskiy Lane, Dolgoprudny, Moscow Region 141701, Russia*

(Received 10 August 2023; revised 13 November 2023; accepted 27 November 2023; published 15 December 2023)

We present results of investigations on the correlated nature of electronic states crossing the Fermi level in $Pb_9Cu(PO_4)_6O$ (also referred to as LK-99) obtained within the DFT+DMFT approach. We found that the band structure in the vicinity of the Fermi level is formed by extremely narrow Cu d states and p states of extra O weakly hybridized with each other. Coulomb correlations between Cu d electrons open the band gap between Cu d_{xz}/d_{yz} and the extra-O p states that form the top of the valence band. Our conclusion is that the extra-oxygen p states play a significant role in the electronic properties and LK-99 cannot be mapped onto a two-band Hubbard model. We also conclude that doping with electrons will turn the stoichiometric $Pb_9Cu(PO_4)_6O$ into a metal, whereas the result of doping with holes is less certain.

DOI: 10.1103/PhysRevB.108.L241111

Introduction. Starting from the first report on the existence of room-temperature superconductivity in $Pb_9Cu(PO_4)_6O$ [1] ("LK-99"), there have been continued attempts to clarify which characteristics of the electronic structure could generate the reported compound properties [2–5]. It is obvious to suggest that the d states of the Cu ion in the formal d^9 electronic configuration are on the Fermi level and the supposed superconductivity is interconnected with them. The crystal structure of $Pb_9Cu(PO_4)_6O$ resembles the most well-known high-T_c superconducting cuprates (HTSC) which have similar Cu-O_2 planes containing Cu^{2+} ions with a d^9 configuration. Hence by analogy with HTSC cuprates, one can assume that LK-99 is a system with strong electron-electron correlations, and density functional theory (DFT) will fail to describe its properties. DFT+U calculations were already presented in Refs. [2–4]. The insulating band structure was obtained in all three works with the existence of long-range ferromagnetic ordering (the long-range magnetic ordering is an artifact of the DFT + U method). The importance of accounting for correlation effects was reported for many high-T_c superconductors with d or f atoms [6–9].

For this study, we have employed the features of the DFT plus dynamical mean-field theory (DFT+DMFT) method to describe the electronic structure of strongly correlated paramagnetic systems, taking into account also a finite electronic temperature.

Methods. We performed DFT+DMFT [10] calculations following the procedure described in Ref. [11]. As a first step, DFT calculations using the QUANTUM ESPRESSO [12] package with pseudopotentials from the standard solid-state pseudopotential library set [13] were performed. The exchange-correlation functional was chosen to be in the Perdew-Burke-Ernzerhof functional adapted for solids (PBEsol) form. The energy cutoff for the plane-wave function and charge density expansion has been set to 50 and 400 Ry, respectively. Integration in the reciprocal space was done on a regular $4 \times 4 \times 5$ k-point mesh in the irreducible part of the Brillouin zone. The convergence criteria used for crystal structure relaxation within DFT are as follows: total energy $< 10^{-8}$ Ry, total force $< 10^{-4}$ Ry/bohrs, pressure < 0.2 kbar.

The Wannier functions $|W_n\rangle$ were utilized for a description of the Cu d and O p states. In the reciprocal space $|W_{n\mathbf{k}}\rangle$ are calculated as a projection of the pseudoatomic orbitals $|\phi_{n\mathbf{k}}\rangle$ onto a subspace of Bloch functions that is defined by setting an energy interval $E_1 \leqslant \varepsilon_i(\mathbf{k}) \leqslant E_2$:

$$|W_{n\mathbf{k}}\rangle \equiv \sum_{E_1 \leqslant \varepsilon_i(\mathbf{k}) \leqslant E_2} |\Psi_{i\mathbf{k}}\rangle\langle\Psi_{i\mathbf{k}}|\phi_{n\mathbf{k}}\rangle.$$

Then the obtained Wannier functions were orthogonalized with the Lödwin symmetric orthogonalization approach [14].

Next, to take into account Coulomb correlations and many-body effects for the constructed small Hamiltonian, the DFT+DMFT approach [10,15] was utilized to solve the Hubbard model (in a density-density approximation). The Coulomb repulsion parameter U which is equal to the F_0 Slater integral and the Hund exchange parameter [for d electrons $J = (F_2 + F_4)/14$] were set to 1.8 eV and $J = 0.7$ eV, correspondingly. DFT+DMFT calculations were performed at an electronic inverse temperature $\beta = 1/k_B T = 40\ \text{eV}^{-1}$, where k_B is the Boltzmann constant

*dmitry@korotin.name

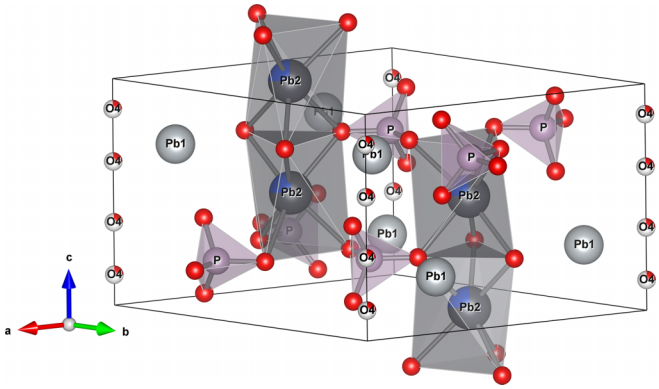

FIG. 1. Crystal structure of $Pb_{10}(PO_4)_6O$. The O4 site (referenced as extra O in the text) has a partial occupation of 0.25. In $Pb_9Cu(PO_4)_6O$, a copper ion substitutes one of the Pb2 ions. Visualized using VESTA [21].

and T is the absolute temperature, which corresponds to 290 K. An effective DMFT quantum impurity problem [16] was solved using the continuous-time quantum Monte Carlo method with the hybridization expansion algorithm [17] as implemented in the package AMULET [18]. We used the maximum entropy method [19] to perform an analytic continuation from imaginary to real frequencies for the single-particle Green's function to obtain spectral functions.

Results. We are still lacking sufficient data regarding the detailed crystal structure of the LK-99 [1] compound. It is known that it was identified as lead apatite $Pb_{10}(PO_4)_6O$ with the $P6_3/m$ space group, wherein a copper ion substitutes one of the Pb ions at position $4f$. Consequently, selecting an appropriate crystal structure for electronic structure calculations is not straightforward.

We started our investigation using the $Pb_{10}(PO_4)_6O$ crystal structure [20], as illustrated in Fig. 1. Importantly, the oxygen ion, which is not part of the PO_4 octahedra, is located at the Wyckoff site $4e$ with a partial occupation of 0.25. In our analysis, we refer to this oxygen ion as "extra O" throughout the text.

The problem of dealing with partial occupation sites (or impurity sites) can be approached in two ways: (1) by calculating large supercells with randomly occupied $4e$ sites by oxygen ions, or (2) by staying within a single cell and avoiding relaxation of the internal atomic positions of the extra-O ion. Avoiding atomic position relaxation in small cells prevents undesirable local distortions that would propagate throughout the crystal due to translation symmetry.

The full band structure and partial densities of states for the extra-O ion for the parent lead apatite compound are shown in Fig. 2. Calculations were done for the experimental crystal structure with only one extra-O ion in the cell. The left panel of Fig. 2 illustrates the presence of narrow energy bands, with a width of approximately 400 meV, situated just below the Fermi level in $Pb_{10}(PO_4)_6O$. These three bands arise from the p states of the extra-O ion. The figure provides evidence that the extra-O ion in the lead apatite can be treated as an impurity, exhibiting minimal interaction with the surrounding ions. Consequently, it forms a distinct set of narrow energy bands.

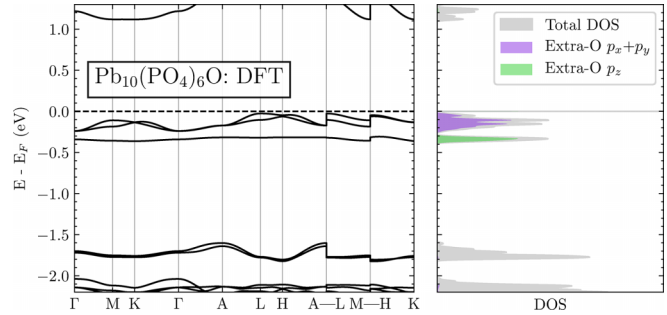

FIG. 2. Energy bands (left panel) and densities of states (right panel) for $Pb_{10}(PO_4)_6O$ obtained within DFT.

The same rationale was used for a copper ion substitution in LK-99, replacing one of the ten Pb ions. The copper ion acts as an impurity that exerts a negligible influence on the average positions of the Pb ions. Consequently, to obtain the structure representing $Pb_{10-x}Cu_x(PO_4)_6O$ ($x = 1$), we substituted one of the lead ions in $Pb_{10}(PO_4)_6O$ with copper. Subsequently, we fixed the atomic positions of Pb, Cu, and extra-O ions and performed relaxation for all other structural parameters, including the crystal shape, volume, and positions of all the remaining atoms. The resulting lattice parameters $a = 9.748$ Å, $c = 7.218$ Å, and $V = 594$ Å^3 agree with the already published data [1,2,4].

The calculated DFT band structure and partial densities of states for the optimized cell of $Pb_9Cu(PO_4)_6O$ are depicted in Fig. 3. The copper ion states also form impuritylike energy bands near the Fermi level, in the energy region slightly higher than the extra-O bands. Two bands crossing the Fermi level are narrower than in previously presented works [2,4] precisely because we did not allow undesirable extra hybridization of Cu and extra-O ions with the nearest-neighbor ion states.

The crystal field of the trigonally distorted oxygen octahedra splits the Cu d shell into a doubly degenerate subshell corresponding to the irreducible representation e_g^σ (d_{xz} and d_{yz} orbitals), doubly degenerate e_g^π subshell ($d_{x^2-y^2}$ and d_{xy} orbitals), and $d_{3z^2-r^2}$ orbital that corresponds to the representation a_{1g}. This splitting is clearly seen in partial densities of states in the right panel of Fig. 3.

Two exceptionally narrow energy bands intersecting the Fermi level correspond primarily to electronic states with Cu d_{xz} and d_{yz} orbital symmetries. These partially filled bands

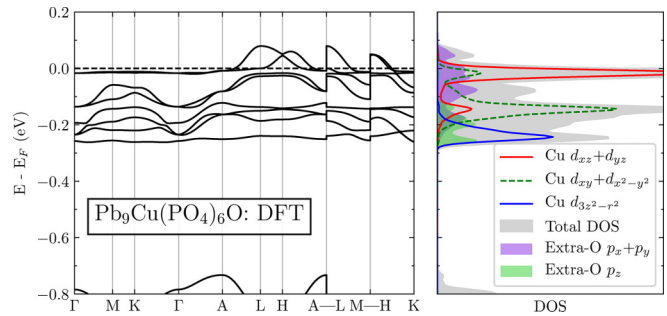

FIG. 3. Energy bands (left panel) and densities of states (right panel) for $Pb_9Cu(PO_4)_6O$ obtained within DFT.

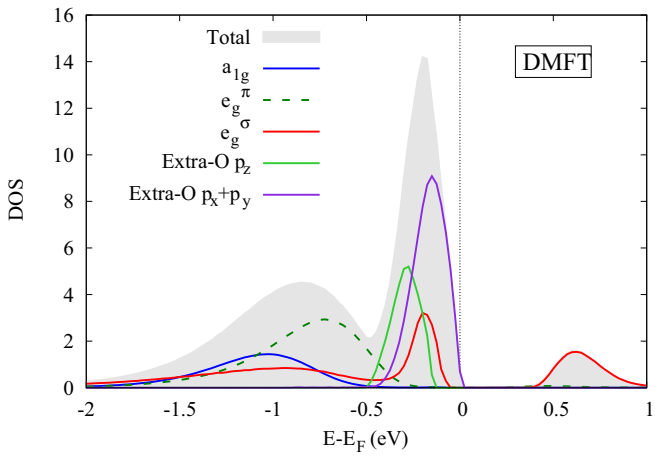

FIG. 4. Orbital-resolved spectral functions of $Pb_9Cu(PO_4)_6O$ calculated within DMFT. Cu a_{1g}, e_g^π, and e_g^π states are shown with solid blue, dark-green dashed, and solid red lines, respectively. The solid green and solid violet lines indicate the extra-O p_z and extra-O $p_x + p_y$ states.

have a width of only about 120 meV, suggesting that strong electronic correlations undoubtedly play a crucial role in their behavior. This fact was already accentuated before [2,4]. These energy bands are almost flat along the $\Gamma-M-K-\Gamma$ path in the Brillouin zone. The Γ, K, and M k points are located in the k_x-k_y plane. The copper energy bands are nondispersive, since the overlap between the orbitals in the *ab* plane of the cell is small.

The two bands within the energy range of $[-0.15, -0.01]$ eV below the Fermi level are attributed to the p_x and p_y orbitals of the extra-O ion. Due to the considerable distance between the Cu and extra-O ions (approximately 5.7 Å), there is minimal overlap between the copper ion orbitals and the extra-O p orbitals, resulting in negligible hybridization between them. Below, there are also Cu $d_{x^2-y^2}/d_{xy}$, extra-O p_z, and Cu $d_{3z^2-r^2}$ related energy bands. The width of the entire band set is about 350 meV.

The eight states mentioned above (five Cu d and three extra-O p) are the minimal basis for the model that could be used for evaluation of the strong Coulomb interaction in $Pb_{10-x}Cu_x(PO_4)_6O$. Using the projection procedure (see Methods), we constructed eight Wannier functions with the symmetry of the corresponding atomic orbitals. Then the Hamiltonian of the Hubbard model Hamiltonian was constructed in the basis of these Wannier functions. The five Wannier functions with Cu d symmetry were considered correlated, and the three O p-like Wannier functions were treated as noncorrelated states.

Next, this small Hamiltonian was solved within the DFT+DMFT method and the obtained spectral functions are shown in Fig. 4. The following experimental data [22] show that under normal conditions, LK-99 demonstrates insulating properties, thereby confirming the predictive outcome obtained in the present Letter. One can see that even such a small $U = 1.8$ eV opens the gap about 0.4 eV and leads to an insulator. The smaller values of U seem physically unjustified, while the larger values, e.g., typical for HTSC cuprates ≈3 eV [23], will not change the picture of the Mott insulator regime.

Recently, several works [24–26] emerged that computed U and J values using the constrained random phase approximation (cRPA) approach. The values obtained for the Coulomb and Hund exchange parameters are consistent with those utilized in our study. Electronic states with e_g^π and a_{1g} symmetry are completely filled. The spectral function of the e_g^σ states demonstrates the appearance of the lower and upper Hubbard bands at -1.1 and 0.6 eV, respectively. The obtained averaged squared magnetic moment is $0.99\mu_B^2$, which corresponds to one hole in doubly degenerate e_g^σ orbitals. The DFT+DMFT results show that taking into account the Coulomb correlation is important since it significantly changes the band structure in the vicinity of the Fermi level obtained in DFT and hence the Fermi-surface topology. Figure 4 shows that the top of the valence band is formed by extra-O $p_x + p_y$ states which are reminiscent of the $Pb_{10}(PO_4)_6O$ since in the case of the absence of Cu the top of the valence band is also formed by extra-O p states. The spectral functions look similar to charge-transfer insulators, i.e., NiO or $LiNiO_2$ [27], but the situation is different in $Pb_9Cu(PO_4)_6O$. In charge-transfer insulators, the energy gap is formed by metal d states and the nearest ligand p states. In LK-99 the states that cross the Fermi level are p states of the extra-O ion which is at least 5.7 Å away from the copper ion. However, if we consider only the composition of the top of the valence band which consists of O p, and the bottom of the conducting band, formed by Cu d states, $Pb_9Cu(PO_4)_6O$ can be identified as a specific example of charge-transfer insulators.

Although our findings reveal the presence of a local magnetic moment on each copper ion, this analysis did not account for long-range magnetic order. Based on these results, two possible scenarios could be proposed: The compound may either behave as a paramagnet due to the thermal disordering of local magnetic moments or it can exhibit ferromagnetic properties. Also, note that a substantial distance between neighboring copper ions makes the possibility of antiferromagnetic ordering low, in contrast to HTSC cuprates. Increasing the Cu-Cu distance weakens the superexchange mechanism responsible for antiferromagnetic (AFM) ordering.

Additionally, if the copper ions form clusters due to their uneven distribution, as proposed in Ref. [22], AFM ordering within these clusters becomes feasible. However, this hypothesis requires further exploration, which is contingent upon the availability of new high-quality structural data.

We assume that in this case of narrow and well-separated bands in the vicinity of the Fermi level, moderate doping with either electrons or holes will not change the electronic spectrum significantly but primarily result in a shift of the Fermi level. For instance, additional electrons will lead to partial occupancy of the upper Hubbard band formed by e_g^σ states, similar to HTSC cuprates, and a transition from the Mott insulator state of stoichiometric $Pb_9Cu(PO_4)_6O$ into a regime of strongly correlated metal [28] will occur, accompanied by a substantial electronic mass enhancement.

On the other hand, the result of hole doping cannot be reliably deduced from these calculations since both the lower Hubbard band formed by Cu e_g^σ states and the p states of the extra O lie below the Fermi level. Additional meticulous examinations of the charge redistribution between these states, which also take into account the response of the crystal lat-

tice, are necessary for determining which of these states will accommodate the holes. This analysis will call the challenge for further investigations.

Conclusion. We investigated the electronic structure and the role of correlation effects in $Pb_9Cu(PO_4)_6O$ within the frame of the DFT+DMFT approach. It was shown that proper accounting for the disorder in the occupation of extra-O and Cu/Pb sites in the parent lead apatite structure is especially important and can result in the appearance of narrow energy bands in the vicinity of the Fermi level in the case of the LK-99 compound. These energy bands originate from the overlap of two band groups, namely Cu d and extra-O p.

Then, using the DFT+DMFT approach, we showed that accounting for Coulomb correlations leads to the band gap opening, which drastically changes the band structure obtained in DFT. However, the physical picture in this compound is much more complicated and cannot be reduced to a Mott insulator on a triangular lattice formed by the Cu d_{xz} and d_{yz} orbitals but could be considered as a specific example of a charge-transfer insulator with a remarkably complicated structure of the valence band of $Pb_9Cu(PO_4)_6O$ formed not by the ligands closest to the Cu ion but by distant extra-O p states.

Acknowledgments. The DFT parts of the study were supported by the Ministry of Science and Higher Education of the Russian Federation (No. 122021000039-4, theme "Electron"). The DMFT results were obtained within the state assignment of the Russian Science Foundation (Project No. 19-72-30043).

[1] S. Lee, J.-H. Kim, and Y.-W. Kwon, The first room-temperature ambient-pressure superconductor, arXiv:2307.12008.

[2] S. M. Griffin, Origin of correlated isolated flat bands in copper-substituted lead phosphate apatite, arXiv:2307.16892.

[3] J. Lai, J. Li, P. Liu, Y. Sun, and X.-Q. Chen, First-principles study on the electronic structure of $Pb_{10-x}Cu_x(PO_4)_6O$ ($x = 0, 1$), J. Mater. Sci. Technol. **171**, 66 (2024).

[4] L. Si and K. Held, Electronic structure of the putative room-temperature superconductor $Pb_9Cu(PO_4)_6O$, Phys. Rev. B **108**, L121110 (2023).

[5] H. Oh and Y.-H. Zhang, S-wave pairing in a two-orbital $t-J$ model on triangular lattice: Possible application to $Pb_{10-x}Cu_x(PO_4)_6O$, arXiv:2308.02469.

[6] V. I. Anisimov, D. M. Korotin, M. A. Korotin, A. V. Kozhevnikov, J. Kuneš, A. O. Shorikov, S. L. Skornyakov, and S. V. Streltsov, Coulomb repulsion and correlation strength in LaFeAsO from density functional and dynamical mean-field theories, J. Phys.: Condens. Matter **21**, 075602 (2009).

[7] A. O. Shorikov, S. L. Skornyakov, V. I. Anisimov, and A. R. Oganov, Electronic correlations in uranium hydride UH_5 under pressure, J. Phys.: Condens. Matter **32**, 385602 (2020).

[8] C. Weber, K. Haule, and G. Kotliar, Strength of correlations in electron- and hole-doped cuprates, Nat. Phys. **6**, 574 (2010).

[9] B. Lilia, R. Hennig, P. Hirschfeld, G. Profeta, A. Sanna, E. Zurek, W. E. Pickett, M. Amsler, R. Dias, M. I. Eremets, C. Heil, R. J. Hemley, H. Liu, Y. Ma, C. Pierleoni, A. N. Kolmogorov, N. Rybin, D. Novoselov, V. Anisimov, A. R. Oganov *et al.*, The 2021 room-temperature superconductivity roadmap, J. Phys.: Condens. Matter **34**, 183002 (2022).

[10] V. I. Anisimov, A. I. Poteryaev, M. A. Korotin, A. O. Anokhin, and G. Kotliar, First-principles calculations of the electronic structure and spectra of strongly correlated systems: Dynamical mean-field theory, J. Phys.: Condens. Matter **9**, 7359 (1997).

[11] D. Korotin, A. V. Kozhevnikov, S. L. Skornyakov, I. Leonov, N. Binggeli, V. I. Anisimov, and G. Trimarchi, Construction and solution of a Wannier-functions based Hamiltonian in the pseudopotential plane-wave framework for strongly correlated materials, Eur. Phys. J. B **65**, 91 (2008).

[12] P. Giannozzi, S. Baroni, N. Bonini, M. Calandra, R. Car, C. Cavazzoni, D. Ceresoli, G. L. Chiarotti, M. Cococcioni, I. Dabo, A. Dal Corso, S. de Gironcoli, S. Fabris, G. Fratesi, R. Gebauer, U. Gerstmann, C. Gougoussis, A. Kokalj, M. Lazzeri, L. Martin-Samos *et al.*, QUANTUM ESPRESSO: A modular and open-source software project for quantum simulations of materials, J. Phys.: Condens. Matter **21**, 395502 (2009).

[13] G. Prandini, A. Marrazzo, I. E. Castelli, N. Mounet, and N. Marzari, Precision and efficiency in solid-state pseudopotential calculations, npj Comput. Mater. **4**, 72 (2018).

[14] P. Löwdin, On the non-orthogonality problem connected with the use of atomic wave functions in the theory of molecules and crystals, J. Chem. Phys. **18**, 365 (1950).

[15] K. Held, I. A. Nekrasov, G. Keller, V. Eyert, N. Blümer, A. K. McMahan, R. T. Scalettar, T. Pruschke, V. I. Anisimov, and D. Vollhardt, Realistic investigations of correlated electron systems with LDA + DMFT, Phys. Status Solidi B **243**, 2599 (2006).

[16] P. Werner and A. J. Millis, Hybridization expansion impurity solver: General formulation and application to Kondo lattice and two-orbital models, Phys. Rev. B **74**, 155107 (2006).

[17] E. Gull, A. J. Millis, A. I. Lichtenstein, A. N. Rubtsov, M. Troyer, and P. Werner, Continuous-time Monte Carlo methods for quantum impurity models, Rev. Mod. Phys. **83**, 349 (2011).

[18] http://www.amulet-code.org.

[19] M. Jarrell and O. Biham, Dynamical approach to analytic continuation of quantum Monte Carlo data, Phys. Rev. Lett. **63**, 2504 (1989).

[20] S. V. Krivovichev and P. C. Burns, Crystal chemistry of lead oxide phosphates: Crystal structures of $Pb_4O(PO_4)_2$, $Pb_8O_5(PO_4)_2$ and $Pb_{10}(PO_4)_6O$, Z. Kristallogr. **218**, 357 (2003).

[21] K. Momma and F. Izumi, VESTA 3 for three-dimensional visualization of crystal, volumetric and morphology data, J. Appl. Crystallogr. **44**, 1272 (2011).

[22] P. Puphal, M. Y. P. Akbar, M. Hepting, E. Goering, M. Isobe, A. A. Nugroho, and B. Keimer, Single crystal synthesis, structure, and magnetism of $Pb_{10-x}Cu_x(PO_4)_6O$, APL Mater. **11**, 101128 (2023).

[23] S.-L. Yang, J. A. Sobota, Y. He, Y. Wang, D. Leuenberger, H. Soifer, M. Hashimoto, D. H. Lu, H. Eisaki, B. Moritz, T. P. Devereaux, P. S. Kirchmann, and Z.-X. Shen, Revealing the Coulomb interaction strength in a cuprate superconductor, Phys. Rev. B **96**, 245112 (2017).

[24] Y. Jiang, S. B. Lee, J. Herzog-Arbeitman, J. Yu, X. Feng, H. Hu, D. Călugăru, P. S. Brodale, E. L. Gormley, M. G. Vergniory,

C. Felser, S. Blanco-Canosa, C. H. Hendon, L. M. Schoop, and B. A. Bernevig, $Pb_9Cu(PO4)_6(OH)_2$: Phonon bands, localized flat band magnetism, models, and chemical analysis, arXiv:2308.05143.

[25] N. Witt, L. Si, J. M. Tomczak, K. Held, and T. O. Wehling, No superconductivity in $Pb_9Cu_1(PO_4)_6O$ found in orbital and spin fluctuation exchange calculations, SciPost Phys. **15**, 197 (2023).

[26] C. Yue, V. Christiansson, and P. Werner, Correlated electronic structure of $Pb_{10-x}Cu_x(PO_4)_6O$, arXiv:2308.04976.

[27] D. M. Korotin, D. Novoselov, and V. I. Anisimov, Paraorbital ground state of the trivalent Ni ion in $LiNiO_2$ from DFT+DMFT calculations, Phys. Rev. B **99**, 045106 (2019).

[28] T. Pruschke, D. L. Cox, and M. Jarrell, Hubbard model at infinite dimensions: Thermodynamic and transport properties, Phys. Rev. B **47**, 3553 (1993).